RSC Advances




ROYAL SOCIETY OF CHEMISTRY

www.rsc.org/advances

Journal Name

RSCPublishing

COMMUNICATION

# Dithieno[3,2-b:2',3'-d]pyran-Containing Organic D-π-A Sensitizers for Dye-Sensitized Solar Cells

Cite this: DOI: 10.1039/xoxxoooooox

Boyang Chu,[a] Hong Wang,[a] Bertrand Xerri,[c] Ka-Ho Lee,[a] Tingbin Yang,[b] Zilong Wang,[a] Zhenyang Lin,[a] Yongye Liang,*[b] Carlo Adamo,*[c,d] Shihe Yang*[a] and Jianwei Sun*[a]

Received ooth January 2012,
Accepted ooth January 2012

DOI: 10.1039/xoxxoooooox

www.rsc.org/

**We describe herein the design and synthesis of two new organic regioisomeric D-π-A sensitizers incorporating dithieno[3,2-b:2',3'-d]pyran (DTP) unit. The dye-sensitized solar cells (DSSCs) based on these two dyes exhibit impressive power conversion efficiency.**

In the past two decades, the development of dye-sensitized solar cells (DSSCs) has emerged as an important research area receiving intense investigations.[1] Among the various dyes as the light harvesters, those based on metal complexes (e.g., Ru- or Zn-complexes) have received considerable attention, and a conversion efficiency as high as 13% has been achieved.[2] In the meanwhile, metal-free organic dye sensitizers have also been a focus of study because of several advantages, such as flexibility in molecular design and absorption tunability as well as low cost.[3,4]

Typical metal-free organic dye molecules employ a D-π-A structure, in which the electron-donor (D), conjugated spacer (π-linker), and electron-acceptor (A) are connected to form the "push-pull" scenario favored for solar cells.[4] Each part of the structure can often have variable influence on the electro-optical properties of the dyes and their performance in devices. As a result, considerable efforts have been paid to the various modifications of these subunits and their structure-performance relationship studies aiming at tuning the HOMO/LUMO energy levels, shifting the absorption spectra, and facilitating electron injection, etc.[1,3-5] Significant progress has been achieved.

Dithieno[3,2-b:2',3'-d]pyran (DTP, Figure 1) has been demonstrated as a useful subunit in polymer OPVs in which low band-gap and high photovoltaic performance have been achieved.[6] However, such a versatile π-linker unit has not been utilized in D-π-A type of dyes for DSSCs. Moreover, we envisioned that this unit has an unsymmetrical pyran unit, so it could also be employed to study the possible dipole moment effect in D-π-A organic dyes.[7] Therefore, we designed the two regioisomeric dyes **1** and **2**, in which the typical triaryl amine (donor) and cyanoacrylic acid (acceptor) are linked with DTP but with opposite orientation. As a result, a small difference in dipole moment between **1** and **2** is expected, with **1** being slightly higher due to the enhancement by a vector component of the local DTP dipole moment that is equidirectional to the donor-to-acceptor dipole moment (Figure 1). It is worth noting that four long alkyl chains (*n*-octyl) are incorporated in both dyes to improve solubility and alleviate aggregation.

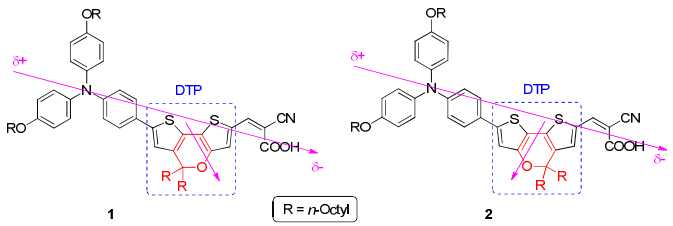


**Fig. 1** Structures of dyes **1** and **2** and the expected DTP influence on dipole moment.

Our synthetic route to the two dyes is shown in Scheme 1. The known bromodithieno[3,2-b:2',3'-d]pyran **3** was employed as the starting compound.[8] The synthesis of dye **1** began with a Suzuki-Miyaura cross-coupling between bromide **3** and arylboronate **4** in the presence of a catalytic mount of $Pd(PPh_3)_4$ to afford the D-π unit **5**. Subsequent introduction of a formyl group on the other side of the DPT linker by Vilsmeier–Haack reaction, followed by installation of the acceptor unit under Knoevenagel condensation conditions, smoothly delivered dye **1**. In a separate route to dye **2**, the starting molecule **3** underwent formylation followed by bromination to form functionalized

DTP **8**. Subsequent sequential installation of the same donor and acceptor units completed the synthesis of dye **2**. Notably, both of the two synthetic routes are expedient.

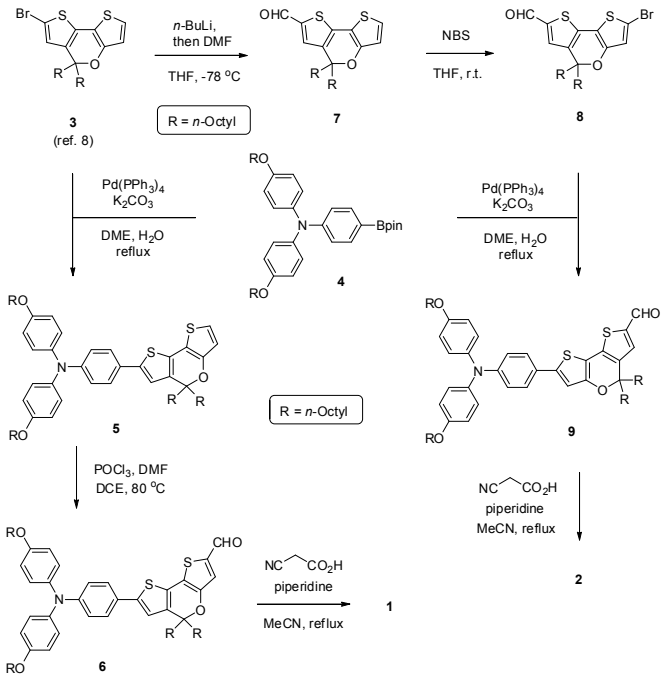


**Scheme 1** Synthesis of **1** and **2**.

The UV-vis absorption spectra of both dyes in $^t$BuOH/MeCN (1:1) and on a porous $TiO_2$ nanoparticle film are depicted in Figure 2, and the corresponding data are included in Table 1. The absorption spectra are similar for both dyes. In the solution phase absorption spectra, there are two prominent bands in the regions 330–400 nm and 400–600 nm. The two dyes have similar $\lambda_{max}$ values (501 vs 496 nm), but dye **2** has a relatively higher molar extinction coefficient (dye **1**: 41500, dye **2**: 51100), suggesting a possible stronger π-π* transition in dye **2**. The slightly weaker absorption of dye **1** is probably due to the slightly weaker donor-to-acceptor coupling, although the orbitals involved (HOMO and LUMO) look qualitatively equivalent. Indeed, it is worth noting that we also carried out computational modeling of the absorption spectra, in which both the absorption intensity and $\lambda_{max}$ value are in very good agreement with the experimental results (see Figure S3 in the SI, using PCM-CAM-B3LYP/6-31+G(d,p)//PBE0/6-31+G(d,p) level). However, the two dyes exhibit very similar absorption on $TiO_2$ film with regard to band wavelength and intensity. Comparing with the absorption in solution, both dyes exhibit obvious hypsochromic shift on the film, indicating some H-aggregation.

The electrochemical properties were studied by cyclic voltammetry (CV) in DMF solutions containing $(^nBu_4N)^+(PF_6)^-$ (0.1 M). Ferrocene was used as an internal standard. The cyclic voltammograms are shown in the SI (Figure S1) and the data are summarized in Table 1. The first oxidation potential ($E_{ox}$), corresponding to HOMO energy, could be attributed to the $TPA^{\bullet+}/TPA^0$ redox process (-5.42eV for dye **1** vs. -5.44eV for dye **2**). The zero-zero energy ($E_{0\text{-}0}$) was estimated from the intersection of absorption and emission spectra (Figure S2), and it was used to calculate the LUMO ($E_{0\text{-}0}$ – HOMO, -3.16eV for dye **1** vs. -3.14 eV for dye **2**). The relatively higher LUMO level and lower HOMO level of dye **2** (i.e., higher band-gap) are probably due to the relatively smaller dipole moment, although the difference is too subtle and an unambiguous conclusion is premature. Furthermore, the more positive oxidation potential relative to the $I^-/I^{3-}$ redox potential (~0.4 V vs NHE) confirms thermodynamically favorable dye regeneration. The LUMO levels are more negative than the conduction band edge of $TiO_2$ (–0.5 V vs NHE), which ensures an efficient electron injection from the excited state of the dye to the $TiO_2$ electrode.[9]

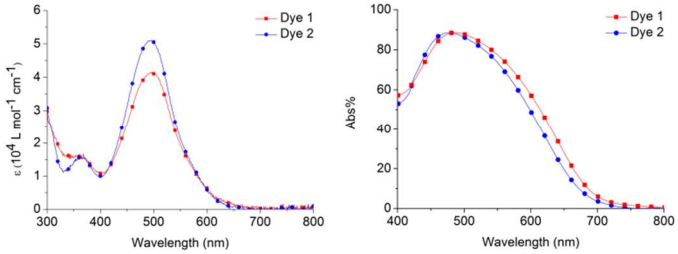


**Fig. 2** UV-vis absorption spectra of dyes **1** (red) and **2** (blue) in solution (left, $^t$BuOH/MeCN = 1:1, 150 μM) and on $TiO_2$ film (right).

**Table 1** Electro-optical parameters of the dyes.

| dye | $\lambda_{abs}$ ($\varepsilon_{max}$ ($10^4$ $M^{-1}$ $cm^{-1}$)) [nm] [a] | $\lambda_{max}$ [nm] [b] | $E_{ox}$ [V] [c] | $E_{0\text{-}0}$ [V] [d] | $E_{ox}$-$E_{0\text{-}0}$ [V] [e] | HOMO/LUMO [eV] [f] |
|---|---|---|---|---|---|---|
| **1** | 501 (4.15) | 485 | 0.92 | 2.26 | -1.34 | -5.42/-3.16 |
| **2** | 496 (5.11) | 476 | 0.94 | 2.30 | -1.36 | -5.44/-3.14 |

[a] Measured in $^t$BuOH/MeCN = 1:1 solution. [b] Absorption maxima on $TiO_2$ film. [c] Measured in DMF. The scan rate is 100 mV $s^{-1}$. The electrolyte is $(^nBu_4N)^+(PF_6)^-$. The working electrode is glassy carbon (reference electrode: $Ag/Ag^+$, calibrated with $Fc/Fc^+$ as an internal reference and converted to NHE by addition of 630 mV). The counter electrode is Pt. [d] $E_{0\text{-}0}$ was estimated from the intersection of the normalized UV-vis spectra and the photo-luminescence spectra. [e] vs NHE. [f] NHE in vacuum was set to -4.5 eV.

We have also carried out DFT calculations to further probe the structural features and the charge excitation behavior of the dyes. The frontier orbitals of the two dyes are shown in the SI (Table S1). The π HOMO orbitals are mainly distributed on the donor side and the π* LUMO orbitals are shifted toward the acceptor side, which is consistent with the charge transfer direction. In addition, the computed HOMO/LUMO gaps are in qualitative agreement with the experimental results obtained from the CV measurement.

Furthermore, we also obtained the electron density distribution map as well as the calculated dipole moments of the dyes (Figure 3). As expected, dye **1** has a relatively larger dipole moment (14.15 D) than dye **2** (13.49 D), but the difference is very small. As shown in the electron density map, the oxygen in the DTP linker pulls electron-density and this pulling effect contributes positively to the overall donor-to-acceptor charge transfer in dye **1** but negatively in dye **2**.

To evaluate the potentials of the new dyes as sensitizers, we fabricated solar cells with an effective area of 0.23 $cm^2$ and the electrolyte composed of 0.05 M $I_2$/0.1 M LiI/0.6 M 1,2-dimethyl-3-*n*-propylimidazolium iodide (DMPImI)/0.5 M 4-*tert*-butylpyridine (TBP) in acetonitrile solution. The typical photocurrent–voltage (*J–V*) curves of the devices under the illumination of AM 1.5 G (100 mW $cm^{-2}$) and the incident photo-to-current conversion efficiency (IPCE) plots of the

cells are presented in Figure 4. The corresponding performance data for the cells are summarized in Table 2. Both dyes exhibit high IPCE performance in the range 300–700 nm, with a maximum value of ~85%. The IPCE with dye **1** in the range 300–500 nm is higher than that with dye **2**, which is consistent with the higher short-circuit current ($J_{sc}$) value of the cell with dye **1** (16.85 mA cm$^{-2}$). However, on the other hand, the open-circuit voltage ($V_{oc}$) with dye **1** (730 mV) is lower than that with dye **2** (765 mV). As a result, the overall power conversion efficiency of the cell with dye **1** (7.69%) is lower than that with dye **2** (8.09%).

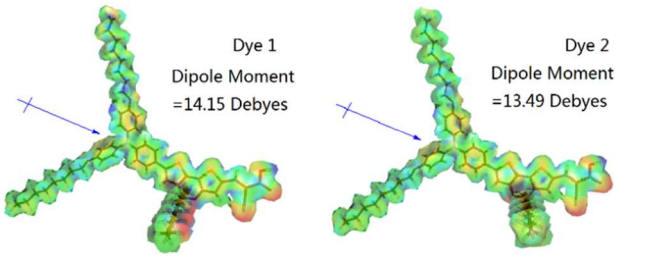


**Fig. 3** Electron density plots and dipole moments for dyes **1** (left) and **2** (right) based on DFT calculation.

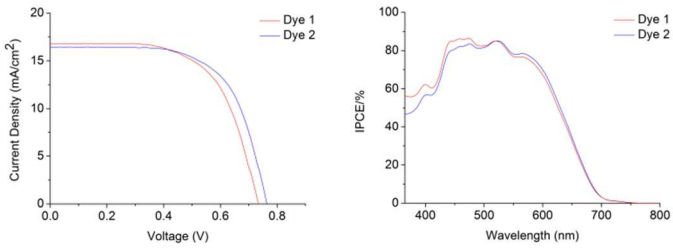


**Fig. 4** Current density-voltage curves (a) and IPCE plots (b) of DSSCs based on dyes **1** and **2**, with CDCA (20 mM) added in both cases.

**Table 2** Device performance parameters of the dyes.

| dye | $V_{oc}$ (mV) | $J_{sc}$ (mA/cm$^2$) | FF | PCE |
|---|---|---|---|---|
| **1** | 733±0.5 | 16.77±0.02 | 0.623±0.002 | 7.68±0.02% |
| **2** | 765±0.5 | 16.45±0.01 | 0.643±0.001 | 8.09±0.01% |

Since $V_{oc}$ outcompetes $J_{sc}$ in influencing the PCE, we decided to examine the possible reasons for the lower $V_{oc}$ for the cell with dye **1**. It is known that $V_{oc}$ can be affected by the conduction band (CB) shift and charge recombination rate in DSSCs.[10] The CB shift determines the quasi-Fermi level of $TiO_2$, which is corresponding to $V_{oc}$ of a DSSC.[11] On the other hand, $V_{oc}$ is also affected by the electron density in titania, which is related to the interfacial recombination rate.[12] The loadings of dyes **1** and **2** were measured and found to be very close to each other ($3.31\times10^{-6}$ mol cm$^{-2}$ vs. $3.19\times10^{-6}$ mol cm$^{-2}$). Therefore, a charge extraction experiment was carried out to further probe these factors.[13] At a certain voltage, the extracted charge with dye **1** is smaller than that with dye **2** (Figure 5a), indicating an upward shift of about 28 mV in the conduction band edge for dye **1**. We also examined the relationship between electron lifetime and the extracted charge (Figure 5b). A longer electron lifetime was observed for dye **2** at a certain extracted charge, implying slower electron recombination. It is known that electron recombination can be accelerated by the presence of a binding site for iodine near the $TiO_2$ surface, and the oxygen atom in the DTP unit can serve as a binding site.[14] Therefore, the relatively faster recombination for dye **1** (vs dye **2**) can be explained by the shorter distance between the oxygen in DTP and the acceptor, which brings the iodide/iodine ion pairs in closer proximity to $TiO_2$. In addition, the position of alkyl side chains for dye **1** and **2** is slightly different. The side chain of dye **2** is closer to the $TiO_2$ surface, which may suppress the electron recombination as well.

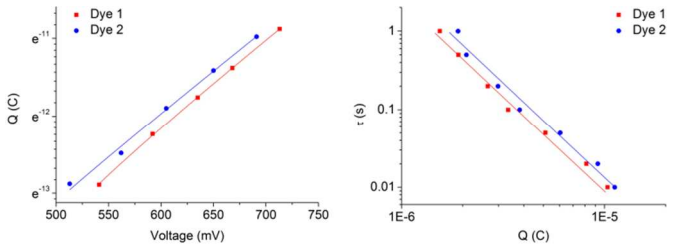


**Fig. 5** Plots of the extracted charge as a function of $V_{oc}$ (a) and the electron lifetime as a function of charge density (b) of DSSCs based on dyes **1** and **2**.

## Conclusions

In summary, we have successfully designed and synthesized two new organic sensitizers (**1** and **2**), which for the first time incorporated dithieno[3,2-b:2',3'-d]pyran (DTP) unit as a π-linker in small molecule organic dyes based on D-π-A structures. By varying the connection orientation of the π-linker, a subtle difference in dipole moments was introduced. DSSCs based on these two dyes have been fabricated and their performance has been evaluated. Although the difference between these two structures and their dipole moments is too subtle to make clear conclusions on their influence, it is noteworthy that the observed power conversion efficiency in our study reached an impressive level (7.69% and 8.09%). Further investigations on dyes with more distinct dipole moment difference will be required.

## Notes and references

[a] Department of Chemistry, The Hong Kong University of Science and Technology, Clear Water Bay, Kowloon, Hong Kong SAR, China. E-mail: sunjw@ust.hk, chsyang@ust.hk

[b] Department of Materials Science and Engineering, South University of Science and Technology of China, Shenzhen 518055, China. E-mail: liang.yy@sustc.edu.cn

[c] Institut de Recherche Chimie Paris, Chimie-Paristech and CNRS, 11 rue P. et M. Curie, F-75005 Paris, France

[d] Institut de Recherche Chimie Paris, Chimie-Paristech and CNRS, 11 rue P. et M. Curie, F-75005 Paris, France; Institut Universitaire de France, 103 Boulevard Saint Michel, F-75005 Paris, France. E-mail: carlo.adamo@chimie-paristech.fr

† We thank Hong Kong RGC for financial support (GRF 606511) and Prof. David Lee Phillips (HKU) for sharing equipment.

Electronic Supplementary Information (ESI) available: Synthesis and characterization of the dyes as well as other experimental details. See DOI: 10.1039/c000000x/

1. For leading references and reviews, see: (*a*) B. O'Regan, M. Grätzel, *Nature* 1991, **353**, 737−740; (*b*) A. Hagfeldt, G. Boschloo, L. Sun, L. Kloo, H. Pettersson, *Chem. Rev.* 2010, **110**, 6595−6663; (*c*) Y. Wu, W. Zhu, *Chem. Soc. Rev.* 2013, **42**, 2039−2058; (*d*) M. Liang, J. Chen, *Chem. Soc. Rev.* 2013, **42**, 3453−3488; (*e*) M. Grätzel, *Acc. Chem. Res.* 2009, **42**, 1788−1798.
2. For selected examples, see: (*a*) S. Mathew, A. Yella, P. Gao, R. Humphrey-Baker, B. F. E. Curchod, N. Ashari-Astani, I. Tavernelli, U. Rothlisberger, M. K. Nazeeruddin, M. Grätzel, *Nat. Chem.* 2014, **6**, 242−247; (*b*) Q. Yu, Y. Wang, Z. Yi, N. Zu, J. Zhang, M. Zhang, P. Wang, *ACS Nano*. 2010, **4**, 6032−6038; (*c*) S.-W. Wang, K.-L. Wu, E. Ghadiri, M. G. Lobello, S.-T. Ho, Y. Chi, J.-E. Moser, F. De Angelis, M. Grätzel, M. K. Nazeeruddin, *Chem. Sci.* 2013, **4**, 2423−2433; (*d*) Y. Cao, Y. Bai, Q. Yu, T. Cheng, S. Liu, D. Shi, F. Gao, P. Wang *J. Phys. Chem. C* 2009, **113**, 6290−6297.
3. For leading reviews and selected examples, see: (*a*) Grätzel, M. *Acc. Chem. Res.* 2009, **42**, 1788−1798; (*b*) Y. Wu, M. Marszalek, S. M. Zakeeruddin, Q. Zhang, H. Tian, M. Grätzel, W. H. Zhu, *Energy Environ. Sci.* 2012, **5**, 8261−8272; (*c*) J. Mao, N. He, Z. Ning, Q. Zhang, F. Guo, L. Chen, W. Wu, J. Hua, H. Tian, *Angew. Chem. Int. Ed.* 2012, **51**, 9873−9876; (*d*) R. Y.-Y. Lin, H.-W. Lin, Y.-S. Yen, C.-H. Chang, H.-H. Chou, P.-W. Chen, C.-Y. Hsu, Y.-C. Chen, J. T. Lin, K.-C. Ho, *Energy Environ. Sci.* 2013, **6**, 2477−2486; (*e*) K. C. D. Robson, K. Hu, G. J. Meyer, C. P. Berlinguette, *J. Am. Chem. Soc.* 2013, **135**, 1961−1971; (*f*) Y. Bai, J. Zhang, D. Zhou, Y. Wang, M. Zhang, P. Wang, *J. Am. Chem. Soc.* 2011, **133**, 11442−11445; (*g*) S. Ito, H. Miura, S. Uchida, M. Takata, K. Sumioka, P. Liska, P. Comte, P. Péchy, M. Grätzel, *Chem. Commun.* 2008, 5194−5196; (*h*) X. Lu, Q. Feng, T. Lan, G. Zhou, Z. Wang, *Chem. Mater.* 2012, 3179−3187; (*i*) Ning, Z.; Fu, Y.; Tian, H. *Energy Environ. Sci.* 2010, **3**, 1170−1181; (*j*) Guo, K.; Yan, K.; Lu, X.; Qiu, Y.; Liu, Z.; Sun, J.; Yan, F.; Guo, W.; Yang, S. *Org. Lett.* 2012, **14**, 2214−2217.
4. For a review, see: A. Mishra, M. K. R. Fischer, P. Bäuerle, *Angew. Chem. Int. Ed.* 2009, **48**, 2474−2499.
5. (*a*) P. Gao, H. N. Tsao, M. Grätzel, M. K. Nazeeruddin, *Org. Lett.* 2012, **14**, 4330−4333; (*b*) W. H. Nguyen, C. D. Bailie, J. Burschka, T. Moehl, M. Grätzel, M. D. McGehee, A. Sellinger, *Chem. Mater.* 2013, **25**, 1519−1525; (*c*) Y. Cui, Y. Wu, X. Lu, X. Zhang, G. Zhou, F. B. Miapeh, W. Zhu, Z.-S. Wang, *Chem. Mater.* 2011, **23**, 4394−4401; (*d*) Q. Feng, X. Jia, G. Zhou, Z.-S. Wang, *Chem. Commun*. 2013, **49**, 7445−7447; (*e*) D. P. Hagberg, J.-H. Yum, H. Lee, F. D. Angelis, T. Marinado, D. M. Karlsson, R. Humphry-Baker, L. Sun, A. Hagfeldt, M. Grätzel, M. K. Nazeeruddin, *J. Am. Chem. Soc.* 2008, **130**, 6259−6266; (*f*) H. Qin, S. Wenger, M. Xu, F. Gao, X. Jing, P. Wang, S. M. Zakeeruddin, M. Grätzel, *J. Am. Chem. Soc.* 2008, **130**, 9202−9203.
6. For an example with DTP in polymer dyes, see: (*a*) J. You, L. Dou, K. Yoshimura, T. Kato, K. Ohya, T. Moriarty, K. Emery, C.-C. Chen, J. Gao, G. Li, Y. Yang, *Nat. Commun.* 2013, **4**, 1446. We are not aware of any D-π-A dyes that contain a DTP unit. For examples containing an analogous cyclopenta[2,1-b;3,4-b']-dithiophene (CPDT) unit, where the oxygen is omitted from DTP, see: (*b*) R. Li, J. Liu, N. Cai, M. Zhang, P. Wang, *J. Phys. Chem. B* 2010, **114**, 4461−4464; (*c*) N. Cai, Y. Wang, M. Xu, Y. Fan, R. Li, M. Zhang, P. Wang, *Adv. Funct. Mater.* 2013, **23**, 1846−1854; (*d*) M. Zhang, Y. Wang, M. Xu, W. Ma, R. Li, P. Wang, *Energy Environ. Sci.* 2013, **6**, 2944−2949.
7. The effect of dipole moment of D-π-A organic dyes the has not been well-studied to the best of our knowledge, although such effect on small molecule and polymer OPVs was documented: (*a*) C. J. Takacs, Y. Sun, G. C. Welch, L. A. Perez, X. Liu, W. Wen, G. C. Bazan, A. J. Heeger, *J. Am. Chem. Soc.* 2012, **134**, 16597−16606; (*b*) B. Carsten, J. M. Szarko, H. J. Son, W. Wang, L. Lu, F. He, B. S. Rolczynski, S. J. Lou, L. X. Chen, L. Yu, *J. Am. Chem. Soc.* 2011, **133**, 20468−20475; (*c*) Y. Liang, L. Yu, *Acc. Chem. Res.* 2010, **43**, 1227−1236; (*d*) S. Chaurasia, C.-Y. Hsu, H.-H. Chou, J. T. Lin, *Org. Electron.* 2014, **15**, 378−390.
8. (*a*) K. Yoshimura, K. Ohya, T. Kato, US Patent, US 2012/0205644, 2012; (*b*) J. Li, X. Deng, Z. Zhang, Y. Wang, Y. Liu, K. He, Y. Huang, Q. Tao, L. Quan, W. Zhu, *J. Polym. Sci. Pol. Chem.* 2012, **50**, 4686−4694.
9. A. Hagfeldt, M. Grätzel, *Chem. Rev*. 1995, **95**, 49−68.
10. (*a*) J. Bisquert, D. Cahen, G. Hodes, S. Rühle, A. Zaban, *J. Phys. Chem. B.* 2004, **108**, 8106−8118; (*b*) M. Planells, L. Pellejà, J. N. Clifford, M. Pastrore, F. D. Angelis, N. López, S. R. Marder, E. Palomares, *Energy Environ. Sci.* 2011, **4**, 1820−1829
11. N. Kopidakis, N. R. Neale, A. J. Frank, *J. Phys. Chem. B* 2006, **110**, 12485−12489.
12. M. Miyashita, K. Sunahara, T. Nishikawa, Y. Uemura, N. Koumura, K. Hara, A. Mori, T. Abe, E. Suzuki, S. Mori, *J. Am. Chem. Soc.* 2008, **130**, 17874−17881.
13. N. W. Duffy, L. M. Peter, R. M. G. Rajapakse, K. G. U. Wijayantha, *J. Phys. Chem. B* 2000, **104**, 8916−8919.
14. (*a*) B. C. O'Regan, K. Walley, M. Juozapavicius, A. Anderson, F. Matar, T. Ghaddar, S. M. Zakeeruddin, C. Klein, J. R. Durrant, *J. Am. Chem. Soc.* 2009, **131**, 3541−3548; (*b*) A. M. Asaduzzaman, G. A. G. Chappellaz, G. Schreckenbach, *J. Comput. Chem.* 2012, **33**, 2492−2497.



 

Organic regioisomeric D-¦Ð-A sensitizers incorporating dithieno[3,2-b:2¡¯,3¡¯-d]pyran (DTP) unit have been designed and evaluated for DSSCs.

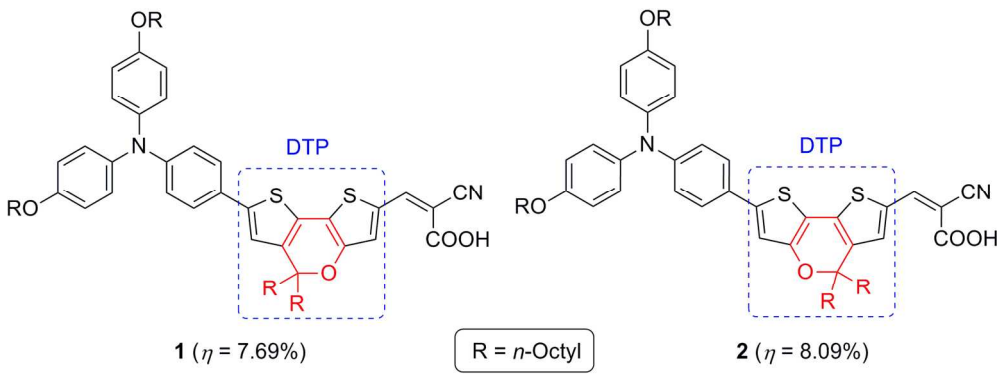


161x60mm (300 x 300 DPI)